17th Brazilian Congress of Thermal Sciences and Engineering
November 25th-28th, 2018, Águas de Lindóia, SP, Brazil

ENCIT-2018-0462
HEAT FLUX AND THERMODYNAMIC PROPERTIES ANALYSIS AT THE STAGNATION POINT AND THE BLUNT REGION OF THE 14-X S SCRAMJET ENGINE

Ana Maria Pereira Lara
Instituto Tecnológico de Aeronáutica, São José dos Campos, São Paulo, 12228-900, Brasil
anamariapereiralara@gmail.com

Paulo Gilberto de Paula Toro
Universidade Federal do Rio Grande do Norte, Natal, Rio Grande do Norte, 59084-100, Brasil
toro11pt@gmail.com

Israel da Silveira Rêgo
Tiago Cavalcanti Rolim
Instituto de Estudos Avançados, São José dos Campos, São Paulo, 12228-001, Brasil
israel.rego@ieav.cta.br
tiagotcr@fab.mil.br

Abstract. *The scramjet engine 14-X S is a technological demonstrator of a hypersonic airbreathing propulsion system based on supersonic combustion. Scramjets are ideal as engines for hypersonic flights, so they are subjected to high heat flux loads, specifically on the leading edge. Thus, this paper applies the normal shock wave relations, the isentropic relations, the Fay and Riddell's theory and the Lees´s theory to study the thermodynamic properties and the aerodynamic heating at the stagnation point and in the blunt region of the 14-X S engine. Two models have been considered for the determination of the thermodynamic properties and for the calculation of the heat flux, being: calorically perfect gas and thermodynamic equilibrium gas. In the blunt region there are the incidence of a normal shock wave that decelerates the flow and increases the pressure and temperature. After the passage through the normal shock wave, the flow will be isentropically decelerated to the stagnation point, increasing again the pressure and the temperature. Increases in the values of thermodynamic properties cause the increase of the heat flux. The highest values of heat flux were found at the stagnation point. After this point, the heat flux had a reduction of about 96% along the blunt region. This showed the importance of the blunt region to soften the values of heat flux that will arrive in the flat sections.*

Keywords: *heat flux, aerothermodynamic, scramjet, hypersonic, blunt body*

1. INTRODUCTION

Scramjet (supersonic combustion ramjet) is a type of propulsion engine that commonly uses the physical phenomena shock waves to get into operation. These shock waves allow the flow to be compressed before the combustion section. Scramjets remove the oxygen necessary for combustion from the atmospheric air, so they do not need to carry it on board. In general, the oxygen corresponds to about 65% of the total weight fraction of the rockets, and, therefore, using scramjets could increase the payload weight fraction.

The 14-X S engine is a technological demonstrator of hypersonic airbreathing propulsion system based on supersonic combustion (scramjet). The 14-X S engine is being developed at the Laboratório de Aerotermodinâmica e Hipersônica Prof. Henry T. Nagamatsu, at the Instituto de Estudos Avançados (IEAv). The main objective of the project is to demonstrate the scramjet technology flying in Earth's atmosphere at 30 km altitude with a Mach number equal to 6.8. The 14-X S engine consists of an inlet composed by a blunt leading edge region and three compression ramps (compression section), by the combustion and expansion sections (Fig. 1).

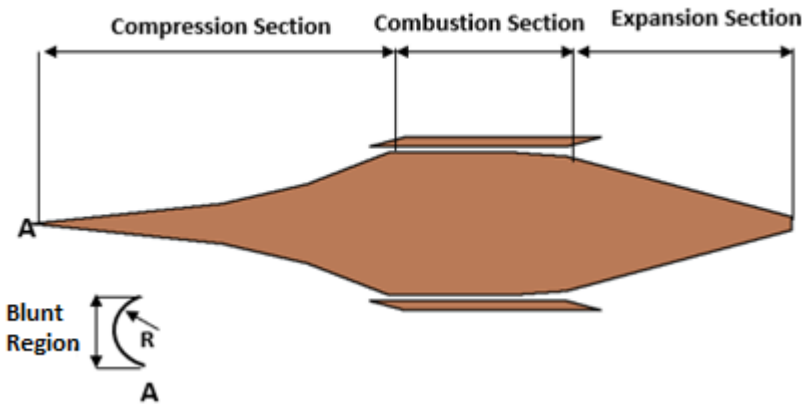

Figure 1. Compression, combustion and expansion section of the 14-X S scramjet engine

In the blunt region of a supersonic flight there is the incidence of a normal shock wave that decelerates the flow and increases the pressure and temperature. After the passage through the normal shock wave, the flow will be decelerated isentropically to the stagnation point, increasing again the pressure and the temperature. Increases in the values of the thermodynamic properties cause the increase of the heat flux. Thus, as scramjets operate in hypersonic speeds, it is possible to have overheating of aerospace vehicles using this technology. Therefore, it is important a heat flux analysis in the blunt region, where the scramjet will have the greatest impact of high heat flux values. In this work, we studied the thermodynamic properties and heat flux at the stagnation point and along the blunt region of the 14-X S engine, considering air as calorically perfect gas and a gas in thermodynamic equilibrium.

2. HEAT FLUX

2.1 Stagnation Point

Using the theory of Fay and Riddell (1958) modified for cylindrical bodies according to Van Driest (1956) it can be to calculate the heat flux at the stagnation point (Eq. (1)) in function of pressure (p), specific mass (ρ), dynamic viscosity (μ), enthalpy (h), Lewis number (L), Prandtl number (Pr) and radius of curvature (R). The flow speed gradient at the stagnation point $\left(\left(\frac{du_e}{dx}\right)_s\right)$ can be obtained by Eq. (2). The subscribers ∞, e, s, D and w refer the properties of the free stream flow, after the normal shock wave, at the stagnation point, of dissociation and in the wall, respectively.

$$q = 0.57Pr^{-0.6}(\rho_s\mu_s)^{0.4}(\rho_w\mu_w)^{0.1}(h_s - h_w)\left[1 + (L^{0.52} - 1)\frac{h_D}{h_s}\right]\left(\frac{du_e}{dx}\right)_s^{0.5} \quad (1)$$

$$\left(\frac{du_e}{dx}\right)_s = \frac{1}{R}\sqrt{\frac{2(p_s - p_\infty)}{\rho_s}} \quad (2)$$

2.2 Blunt Region

In the Fig. 2 is represented the angular variation (θ) from the stagnation point to the beginning of the flat sections (first compression ramp,θ_C) in a blunt region with radius of curvature R. The angle θ varies between 0° and 90° - θ_C.

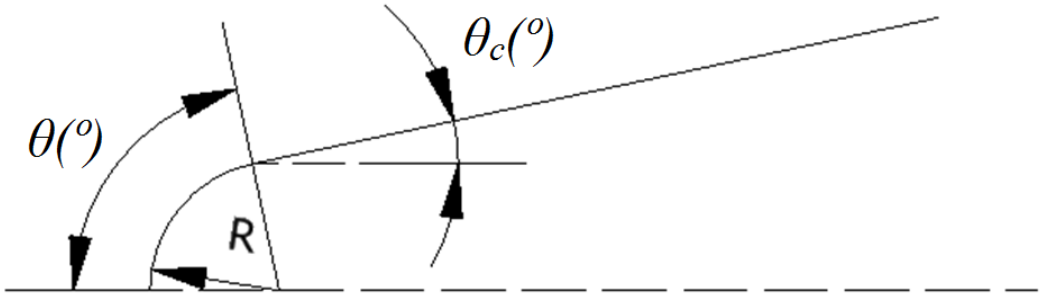

Figure 2. Blunt region and first compression ramp of the 14-X S engine

The calculation of the heat flux outside the stagnation point of the blunt region ($\dot{q}$) is done using Lees (1956). The Lees's theory (Eq. (3) and (4)) is dimensioned as a function of the geometric position (θ) in relation with the heat flux at the stagnation point ($\dot{q}_0$), Mach number of the freestream flow (M_∞) and the ratio between specific heats (γ).

$$\frac{\dot{q}}{\dot{q}_0} = \frac{2\theta sen\theta\{\left[1-\frac{1}{\gamma M_\infty^2}\right]cos^2\,\theta+\frac{1}{\gamma M_\infty^2}\}}{[D(\theta)]^{0.5}} \tag{3}$$

$$D(\theta) = \left[1-\frac{1}{\gamma M_\infty^2}\right]\left[\theta^2-\frac{\theta sen4\theta}{2}+\frac{1-cos4\theta}{8}\right]+\frac{4}{\gamma M_\infty^2}\left[\theta^2-\theta sen2\theta+\frac{1-cos2\theta}{2}\right] \tag{4}$$

3. THERMODYNAMIC PROPERTIES

3.1 Normal Shock Wave

When an aerospace vehicle with blunt frontal geometry travels in the Earth's atmosphere at supersonic speed, a bow shock wave is established at the stagnation point of the aerospace vehicle (Fig. 3), the center of this bow shock wave can be represented by a normal shock wave which causes the deceleration and compression of the flow to subsonic speed and increase of pressure (p), specific mass (ρ) and temperature (T).

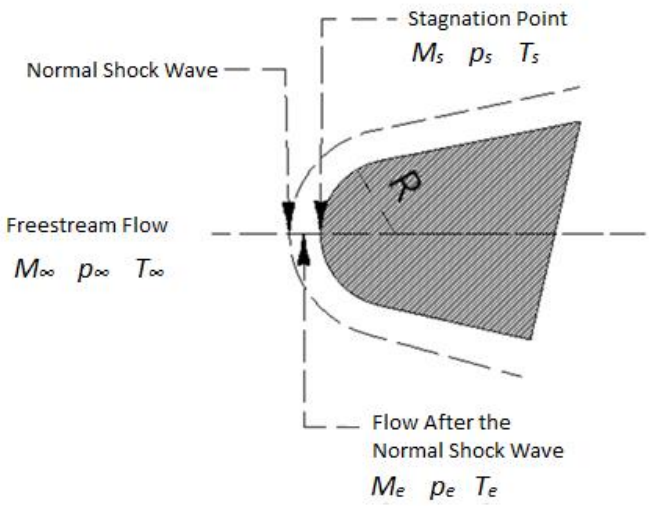

Figure 3. Free stream flow, normal shock wave and stagnation point of a blunt body

The thermodynamic properties after the normal shock wave are obtained using the normal shock relations (ANDERSON JR, 2003), Eq. (5), (6), (7) and (8).

$$M_e{}^2 = \frac{1 + \left[\left(\frac{\gamma - 1}{2}\right)\right] M_\infty^2}{\gamma M_\infty^2 - \left(\frac{\gamma - 1}{2}\right)} \tag{5}$$

$$\frac{p_e}{p_\infty} = 1 + \frac{2\gamma}{\gamma + 1}(M_\infty^2 - 1) \tag{6}$$

$$\frac{\rho_e}{\rho_\infty} = \frac{(\gamma + 1)M_\infty^2}{2 + (\gamma - 1)M_\infty^2} \tag{7}$$

$$\frac{T_e}{T_\infty} = \frac{p_e}{p_\infty}\frac{\rho_\infty}{\rho_e} \tag{8}$$

3.2 Isentropic Flow after the Normal Shock Wave

After that the flow is decelerated irreversibly (with increase of the entropy), due the passage of the flow through the normal shock wave, the flow is decelerated to zero speed, isentropically, until at the stagnation point (Fig. 3). The pressure (p_s), specific mass (ρ_s) and temperature (T_s) of the flow at the stagnation point are obtained using isentropic relations, Eq.(9), (10) and (11), (ANDERSON JR, 2003).

$$\frac{p_s}{p_e} = \left(1 + \frac{\gamma - 1}{2} M_e^2\right)^{\frac{\gamma}{\gamma - 1}} \tag{9}$$

$$\frac{\rho_s}{\rho_e} = \left(1 + \frac{\gamma - 1}{2} M_e^2\right)^{\frac{1}{\gamma - 1}} \tag{10}$$

$$\frac{T_s}{T_e} = 1 + \frac{\gamma - 1}{2} M_e^2 \tag{11}$$

4. METHODOLOGY

4.1 Stagnation Point

In the calculation of the heat flux at the stagnation point are considered two cases: calorically perfect gas and gas in thermodynamic equilibrium. Initially, it is obtained the thermodynamic properties after the normal shock wave using normal shock relations. After, the isentropic relations are used to calculate the properties at the stagnation point. After the calculation of the properties, the expression of Fay and Riddell (1958) is applied to determine the heat flux (Fig. 4).

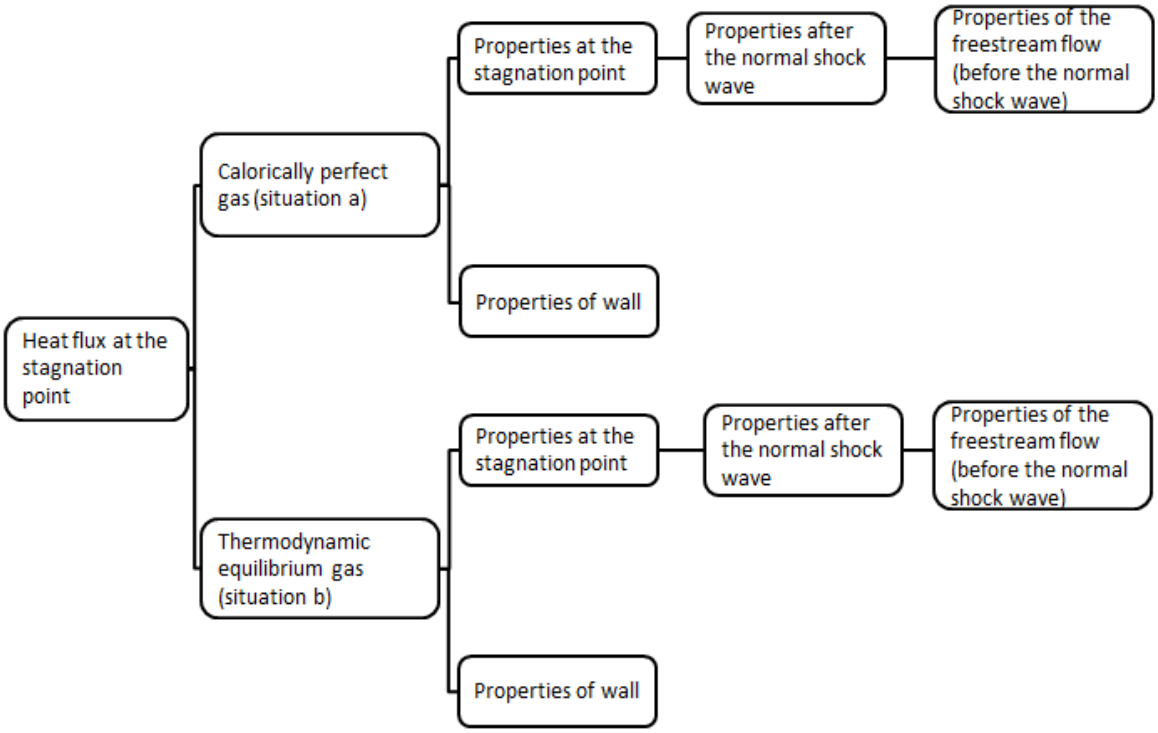

Figure 4. Flowchart of calculations of the heat flux at the stagnation point of the 14-X S engine

Fay and Riddell (1958) assume that the number of Lewis is constant across the boundary layer considering its value varying between 1 and 2. By the Reynolds Analogy it can be assumed that the thermal diffusivity (α) and the mass diffusivity (D_{AB}) are equals. Thus, $\alpha = D_{AB}$, and by Eq. (12), the Lewis number is 1.

$$L = \frac{\alpha}{D_{AB}} \tag{12}$$

The pressure across the boundary layer, starting from the surface to the end of the boundary layer, is assumed constant, so $p_w = p_s$. Therefore, starting from the equation of state (Eq. (13)), the specific mass of the air adjacent to the wall can be calculated by Eq. (14), (where R_G is the gas constant).

$$p = \rho R_G T \tag{13}$$

$$\frac{\rho_w}{\rho_s} = \frac{T_s}{T_w} \quad \therefore \quad \rho_w = \left(\frac{T_s}{T_w}\right) \times \rho_s \tag{14}$$

Fay and Riddell (1958) consider the temperature in the wall varying between 300 K and 3000 K. Assume in this paper an arbitrary value of 300 K.

The dynamic viscosity can be determined by the Sutherland equation:

$$\frac{\mu}{\mu_r} = \left(\frac{T}{T_r}\right)^{\frac{3}{2}} \left(\frac{T_r + S}{T + S}\right), \tag{15}$$

where μ_r e T_r are determined as a function of sea level values, given by μ_r= 1.789 x 10^{-5} (N.s/m^2) and T_r= 288K. The constant S is 110 K.

The number of Prandtl (Pr) is defined by Eq. (16) in function of the dynamic viscosity (μ), the specific heat at constant pressure (c_p) and the thermal conductivity (k). Fay and Riddell (1958) assume that Pr = 0.71.

$$Pr = \frac{\mu c_p}{k} \tag{16}$$

4.2 Blunt Region

Two cases are considered in calculation the heat flux in the blunt region: calorically perfect gas and thermodynamic equilibrium gas. The heat flux is calculated using Lees's theory (1956), which relates the heat flux obtained at the stagnation point and the angular variation along the blunt region. Thus, it is not necessary to calculate the properties along the whole blunt region. In the case of 14-X S engine the maximum angle (θ_c) is 84.5°. This value is reached at the intersection of the blunt region with the first ramp (Fig. 2), where the flat plate (1st ramp) is tangent to the blunt region (circumference).

The boundary layer is established near at the stagnation point, the boundary layer thickness is zero at the stagnation point, and therefore the boundary layer effects are not considered in the calculations. Furthermore, for practical body shapes the viscous terms in the Navier-Stokes equations can be neglected, so the flow can be approximately represented by an inviscid flow solution having the body shape as boundary conditions. This solution is a good approximation, and it is not affected by the Reynolds number. The flow near the wall can be analyzed by a boundary-layer type of analysis using appropriate boundary conditions. This approach permits the determination of the heat transfer in the region of the nose also at very low Reynolds numbers without the necessity of solving the Navier-Stokes equations.

5. RESULTS AND DISCUSSION

5.1 Thermodynamic Properties

The Tab. 1 shows the thermodynamic properties after the normal shock wave for the calorically perfect gas (case a) and for thermodynamic equilibrium (case b). It is observed in both cases that the normal shock wave reduces the speed of flow to subsonic, and increases the thermodynamic properties (pressure, temperature, specific mass and speed of sound).

Table 1. Thermodynamic properties of the flow after the normal shock wave

Case	M_e	T_e (K)	p_e(kPa)	ρ_e (kg/m^3)	u_e(m/s)	a_e(m/s)	γ_e
a	0.40	2.249	64.37	0.0996	379	950	1.40
b	0.38	1.992	66.31	0.1155	326	862	1.27

It can be observed that the temperature is lower in the equilibrium case when compared with the calorically perfect case. For a calorically perfect gas, the kinetic energy of a flow ahead of the shock is mostly converted to translational and rotational molecular energy behind the shock. On the other hand, for a thermally perfect and/or chemically reacting gas, the kinetic energy of the flow, when crossing the shock wave, is partitioned among other molecular modes of energy, or is consumed by endothermic chemical reactions involved, if any. Hence, the temperature (which is a measure of translational energy only) is lower for the equilibrium case.

In Tab. 2, it is shown the thermodynamic properties at the stagnation point considering (a) calorically perfect gas and (b) thermodynamic equilibrium gas. It can be verified that in both cases the flow is decelerated isentropically to the stagnation point, with an increase in the thermodynamic properties (pressure, temperature and specific mass). The equilibrium case has a higher temperature value and a lower pressure value compared with the calorically perfect case.

Table 2. Thermodynamic properties of the flow at the stagnation point

Case	T_s(K)	p_s(kPa)	ρ_s(kg/m^3)	a_s(m/s)	μ_s(N.s/m^2)	h_s (MJ/kg)	γ_s
a	2.321	71.82	0.1077	966	6.70 x 10^{-5}	2.33	1.40
b	2.031	72.68	0.1241	864	6.23 x 10^{-5}	2.03	1.28

In Tab. 3, it is shown the thermodynamic properties of the flow on the wall surface considering (a) calorically perfect gas and (b) thermodynamic equilibrium gas. It was considered an arbitrary value for the temperature on the wall surface of 300 K. The properties for both cases have close values.

Table 3. Thermodynamic properties of the flow on the wall surface

Case	T_w(K)	p_w(kPa)	μ_w (N.s/m^2)	h_w(kJ/kg)
a	300	71.82	1.8463 x 10^{-5}	301.35
b	300	72.68	1.8463 x 10^{-5}	303.42

5.2 Heat Flux

The heat flux calculated at the stagnation point was 4,408 kW/m^2, considering the calorically perfect case, the highest value found along the surface of the scramjet, see Fig. 5. This happened due the deceleration to subsonic speed caused by the normal shock wave, and then by the isentropic deceleration to the stagnation point. These decelerations cause the increase of thermodynamic properties (pressure, temperature, specific mass and speed of sound), and consequently the increase of the heat flux at the stagnation point. The heat flux at the stagnation point was 3,742 kW/m^2 for the thermodynamic equilibrium case, i.e. 15.1% less than the calorically perfect case. The heat flux decreases after the stagnation point, presenting in the region of intersection with the first ramp with a value of 176 kW/m^2 for the case of thermodynamic equilibrium and a value of 196 kW/m^2 for the case of the calorically perfect gas. This shows that the blunt region has high efficiency on reducing the value of the heat flux distribution, approximately 95.65% (calorically perfect case).

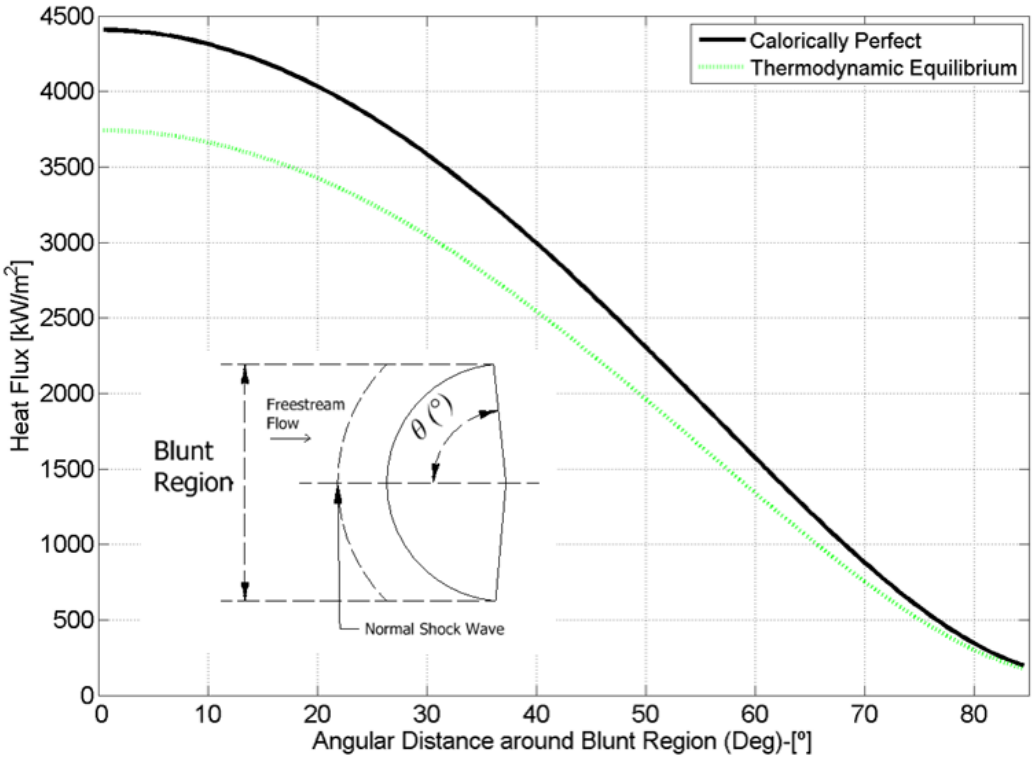

Figure 5. Heat flux along the angular distance around the blunt region of the 14-X S engine

6. CONCLUSION

This paper showed the calculations of the thermodynamic properties and the heat flux along the blunt region of the Technological Demonstrator scramjet 14-X S for calorically perfect and thermodynamic equilibrium gas cases. The calculations were done considering a flight Mach number 6.8 at an altitude of 30 km. The Fay and Riddell's theory and

the Lees's theory were used to calculate the heat flux. The theory of normal shock waves and isentropic relations were used to calculate the thermodynamic properties in the blunt region. The flow is decelerated to subsonic speed after the normal shock wave, and then decelerated isentropically to the stagnation point. These decelerations cause the increase of thermodynamic properties (pressure, temperature, specific mass and speed of sound). The temperature at the stagnation point is lower in the equilibrium case compared to the calorically perfect case. This happens due to the excitation of the vibrational modes of the oxygen and nitrogen molecules present in air. The pressure at the stagnation point is greater in the case in equilibrium when compared to the calorically perfect case. At the stagnation point, it was calculated heat flux of 4,408 kW/m^2 (calorically perfect gas), the highest value of heat flux along the surface of the 14-X S engine. The blunt region was responsible for the greatest reduction of the heat flux distribution (approximately 95.65%). These results shall be used in future works, when defining which materials are the most adequate to withstand the high heat fluxes presented in the 14-X S engine operation.

7. ACKNOWLEDGEMENTS

The first author would like to express gratitude to CAPES and to the project COMAER PROPHIPER 14-X for financial support to graduate student.

8. REFERENCES

ANDERSON JR, J. D. **Modern Compressible Flow:** With Historical Perspective. 3. ed. New York: McGraw-Hill, 2003.
FAY, J. A.; RIDDELL, F. R. Theory of Stagnation Point Heat Transfer in Dissociated Air. **Journal of the Aeronautical Sciences**, v. 25, n. 2, p. 73-85, Feb 1958.
LEES, L. Laminar Heat Transfer Over Blunt-Nosed Bodies at Hypersonic Flight Speeds. **Journal of Jet Propulsion**, p. 259-274, April 1956.
VAN DRIEST, E. R. The Problem of Aerodynamic Heating. **Aeronautical Engineering Review**, p. 1519-1541, Oct 1956.

9. RESPONSIBILITY NOTICE

The authors are the only responsible for the printed material included in this paper.